

# Aluminum coating by fluidized bed chemical vapor deposition on austenitic stainless steels AISI 304 and AISI 316

Jose Luddey Marulanda-Arevalo <sup>a</sup>, Saul Castañeda-Quintana <sup>b</sup> & Francisco Javier Perez-Trujillo <sup>c</sup>

<sup>a</sup> Universidad Tecnológica de Pereira, Pereira - Colombia. [jlmarulanda@utp.edu.co](mailto:jlmarulanda@utp.edu.co)

<sup>b</sup> Universidad Complutense de Madrid, Madrid - España. [sicastan@quim.ucm.es](mailto:sicastan@quim.ucm.es)

<sup>c</sup> Universidad Complutense de Madrid, Madrid - España. [fjperez@quim.ucm.es](mailto:fjperez@quim.ucm.es)

Received: January 25th, 2014. Received in revised form: August 20th, 2014. Accepted: September 8th, 2014.

## Abstract

Aluminum coatings were deposited on stainless steels AISI 304 and AISI 316 at a temperature range from 560 to 600°C by CVD-FBR, using a bed consisting of a 10% aluminum powder and 90% of bed inert (alumina) which was fluidized with Ar and an activator mixture of hydrochloric acid with hydrogen (HCl/H<sub>2</sub>). The coating without heat treatment includes the follow species: Al<sub>13</sub>Fe<sub>4</sub>, Fe<sub>2</sub>Al<sub>5</sub>, FeAl<sub>2</sub> and Al<sub>5</sub>FeNi for both steels. In addition, the heat treatment causes the aluminum to diffuse into the substrate and the iron diffuse towards the surface of the coating, making the transformation of previous existing compounds to FeAl, Fe<sub>2</sub>Al<sub>5</sub>, FeAl<sub>2</sub>, Al<sub>0.99</sub>Fe<sub>0.99</sub>Ni<sub>0.02</sub>, AlNi and Fe<sub>2</sub>AlCr. Thermodynamic simulation was conducted with the Thermo-Calc software to obtain information of the possible composition and amount of deposited material, for selected conditions. The specimens coated and uncoated were exposed at 750 °C in an atmosphere where the vapor was transported to the samples using a N<sub>2</sub> flow of 40 ml/min plus 100% water vapor (H<sub>2</sub>O). The two uncoated substrates behaved differently, since the steel AISI 304 performed well and gained little weight (0.49 mg/cm<sup>2</sup>), compared to the steel AISI 316 that lost too much weight (25.4 mg/cm<sup>2</sup>). Coated steels gained little weight during thousand hours of exposure (0.26 mg/cm<sup>2</sup>) and support very well the corrosive attack compared to uncoated substrates.

**Keywords:** Aluminum, Chemical vapour deposition, Coating, Corrosion, Fluidized bed, High temperature, Inter-metallic coatings, Oxidation

## Recubrimientos de aluminio por deposición química de vapor en lecho fluidizado sobre aceros inoxidables austeníticos AISI 304 y AISI 316

### Resumen

Los revestimientos de aluminio fueron depositados sobre aceros inoxidables AISI 304 y AISI 316 en el rango de temperatura de 560 a 600 °C por deposición química de vapor en lecho fluidizado (CVD - FBR). Se utilizó un lecho que consistía en 10 % de aluminio en polvo y 90 % de lecho inerte (alúmina), el cual fue fluidizado con Ar y como gases activadores se utilizó una mezcla de ácido clorhídrico con hidrógeno (HCl/H<sub>2</sub>). En el recubrimiento sin tratamiento térmico están las siguientes especies: Al<sub>13</sub>Fe<sub>4</sub>, Fe<sub>2</sub>Al<sub>5</sub>, FeAl<sub>2</sub> y Al<sub>5</sub>FeNi, las cuales están presentes para ambos aceros. Además, el tratamiento térmico provoca la difusa de aluminio hacia el sustrato y la difusa de hierro del sustrato hacia la superficie del recubrimiento, haciendo la transformación de los compuestos anteriores a FeAl, Fe<sub>2</sub>Al<sub>5</sub>, FeAl<sub>2</sub>, Al<sub>0.99</sub>Fe<sub>0.99</sub>Ni<sub>0.02</sub>, AlNi y el Fe<sub>2</sub>AlCr. Se realizó la simulación termodinámica con el software Thermo - Calc para obtener información de la posible composición y la cantidad de material depositado, para condiciones seleccionadas. Las muestras recubiertas y sin recubrir, se expusieron a 750 °C en una atmósfera donde el vapor agua se transporta a las muestras usando un flujo de N<sub>2</sub> de 40 ml/min, más 100 % vapor de agua (H<sub>2</sub>O). Los dos sustratos sin revestir se comportaron de manera diferente, ya que el acero AISI 304 soportó bien el ataque y ganó poco peso (0.49 mg/cm<sup>2</sup>), en comparación con el acero AISI 316 que perdió mucho peso (25.4 mg/cm<sup>2</sup>). Los aceros recubiertos ganaron poco de peso durante las mil horas de exposición (0.26 mg/cm<sup>2</sup>) y soportaron muy bien el ataque corrosivo en comparación con sustratos sin recubrimiento.

**Palabras clave:** Alta temperatura, Aluminio, Corrosión, Deposición química de vapor, Lecho fluidizado, Oxidación, Recubrimiento, Recubrimientos Inter-metálicos.

## 1. Introduction

Many industries use coatings to prolong the life of their

products, increase efficiency and reduce production costs and maintenance. Reliability and efficiency of these layers require the appropriate selection and correct application of

these coatings for a successful operation. The above would increase the useful life of machine components and facilities, leading to savings on global consumption of materials [1-3].

Coatings obtained by chemical vapor deposition (CVD) are one of the alternatives for surface protection against corrosion and wear. CVD consists of the reaction of a mixture of gases inside a vacuum chamber to deposit thin layers of different materials [4, 5]. Inside a reaction chamber, the substrate is exposed to one or more volatile precursor gases, which in turn react or decompose on the substrate surface and deposit a solid coating in a thin layer, and by-products of reaction can produce volatile compounds that are removed towards the outside by a flow of gas passing through the reaction chamber [6,7].

Chemical vapor deposition by fluidized bed (CVD-FBR) is a variant of the chemical vapor deposition that combines the advantages of thermal activation by heating and the fluidized bed. Advantages of fluidized beds, such as the high transfer mass and heat among the gas, the bed and the samples immersed in the reactor, allowing a more uniform temperature and very good mixture of reactive gases with fluidized particles. CVD-FBR achieves a high degree of reaction for all species activated in bed, because of the excellent contact between the solid particles and the fluidization gas [8-10]. This helps to reduce the temperature and operation time compared to other processes such as pack cementation [5,9]. In addition, working at atmospheric pressure can save the purchase of expensive vacuum equipment, and cover large parts "*in-situ*", meaning an advantage from the economic point of view.

The use of aluminum layers is an effective way to increase corrosion resistance of steels. This protection is obtained by forming a surface film of alumina ( $\text{Al}_2\text{O}_3$ ). The coating grows by internal diffusion of aluminum; while iron and chromium diffuse outward [11-13]. The inherent property of aluminum to form stable layers of  $\text{Al}_2\text{O}_3$  in atmospheres containing oxygen is well known and it has been adapted for surface enrichment of steel components that operate in aggressive environments at high temperature, since alumina has excellent mechanical properties and good chemical stability at high temperature [14-16].

## 2. Experimental procedure

Specimens (20 mm x 6 mm x 2 mm) of austenitic stainless steels AISI 304 and AISI 316 were used. For this study of aluminum deposition, the specimens were machined and polished with emery paper from No. 100 to No. 600 and then cleaned in ultrasonic ketone bath for 10 minutes. Finally the aluminum coating was deposited by CVD-FBR. Thermodynamic simulations were performed to investigate the better conditions for deposition of aluminum coatings in CVD-FBR using Thermo Calc software® [17]. The calculations are based on free Gibbs energy minimization method and mass conversion rule. To define the gaseous species and solid species, the thermodynamic simulation was performed using the software Thermo-Calc, combining two databases from Scientific Group Thermo-data Europe: SSOL2 and SSUB3. The research of the main

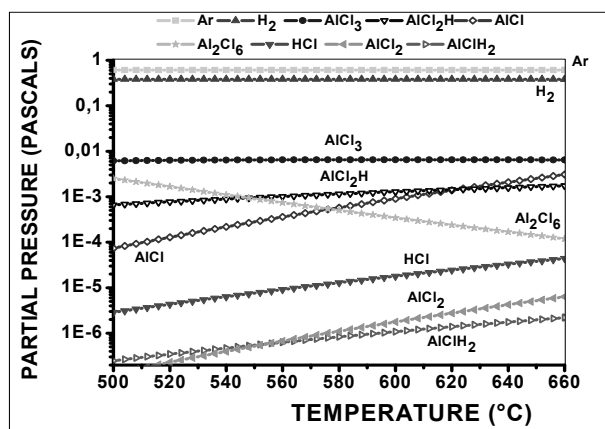
precursor gases and phases formed at equilibrium at the temperature range 500 – 660 °C provides an understanding of the reactions during the deposition. The schematic diagram of the CVD-FBR system used in this work is described in [18,19].

The reactor was made of quartz tube and was heated by an external furnace. The bed used was composed of a mix of 10 wt% aluminum powder with 99.5% of purity and 400  $\mu\text{m}$  particle size as donor, plus 90 wt% alumina ( $\text{Al}_2\text{O}_3$ ) as inert bed. The powder mixture was fluidized by Ar gas (99.999 % purity) with hydrogen chloride plus hydrogen ( $\text{HCl} + \text{H}_2$ ). These gases are used as activators for generating aluminum precursor. The chamber reaction temperature was controlled by a thermocouple introduced into fluidized bed and the samples were suspended above the fluidized bed during the aluminum deposition. The bed was fluidized with Ar between 300 and 3000 ml/min and as activator was used a mixture of  $\text{HCl}/\text{H}_2$  at a ratio from 1/15 to 1/20. These tests were performed at a temperature range from 560 to 600°C with exposure times from 45 minutes to 2.5 hours on different types of austenitic stainless steels. After deposition of the CVD-FBR coatings, a diffusion heat treatment was performed under argon flow at 750 °C for 2 h, followed by cooling into the furnace under an atmosphere of Ar gas. The morphology study of the aluminum layers was carried out using metallographic preparation followed by scanning electron microscopy (SEM-JEOL JM-6400). The composition was studied by energy dispersed X-ray spectroscopy (EDAX) and the structure was studied by X-ray diffraction (XRD-PHILIPS X (PERT MPD)) through the modes  $\theta$ -2 $\theta$  and grazing angle in order to identify phase composition of coated samples. Standard metallographic preparation was performed on samples prior to cross-section observations. The specimens were exposed at 750 °C in an atmosphere where the vapor was transported to the samples by a flow of  $\text{N}_2$  of 40  $\text{ml}\cdot\text{min}^{-1}$  plus 100% water vapor ( $\text{H}_2\text{O}$ ). The test was conducted up to 1000 hours, taking samples at 200, 400, 600, 800 and 1000 hours. After each exposure, the samples were cooled inside the furnace and the samples were weighted on an analytical balance with precision of  $10^{-5}\text{g}$ .

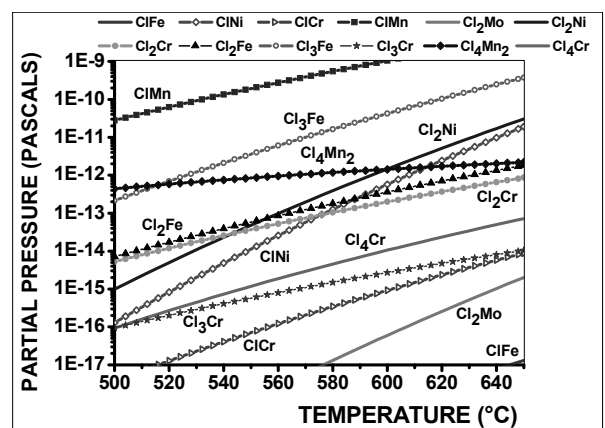
## 3. Results and discussion

### 3.1. Aluminum coatings

Reactions were studied in the aluminum bed and the gases activators  $\text{HCl} + \text{H}_2$ , to obtain information of the deposition process of aluminum layers by CVD-FBR. In the results obtained by the thermodynamics simulation, it was found that the precursors  $\text{Al}_3\text{Cl}$  and  $\text{AlCl}$  were formed at the temperature range from 500 – 660 °C. It has also been observed that  $\text{AlCl}$  is the most important precursor in the formation mechanism of the aluminum layer, since  $\text{Al}_3\text{Cl}$  is very stable. Fig. 1a shows the thermodynamic simulation of aluminum deposition process on AISI 304 stainless steel, and also reports the partial pressures of the gaseous phase as a function of temperature. It is clear that the aluminum deposition is carried out mainly by the following chlorides  $\text{AlCl}_3$ ,  $\text{AlCl}_2\text{H}$ ,  $\text{Al}_2\text{Cl}_6$  and  $\text{AlCl}$  and in smaller proportion



a) Formation of aluminum chlorides



b) Formation of metal chlorides

Figure 1. Thermodynamic simulation of the formation of precursors of the deposition of aluminum by chemical vapor deposition in Fluidized bed reactors. Source: The Authors

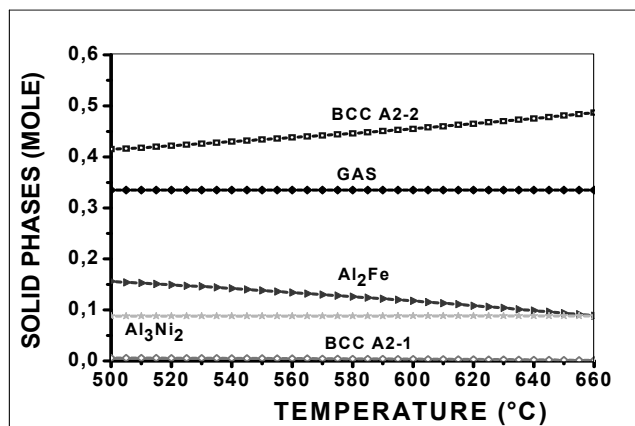
by  $AlClH_2$  and  $AlCl_2$ . The most stable species are  $AlCl_2H$  and  $AlCl_3$ . The only species whose partial pressure decreases with increase of temperature is  $Al_2Cl_6$  and above  $575^\circ C$  the partial pressure is lower than that of  $AlCl$ . Fig. 1b shows the temperature versus the partial pressure for chlorination of iron, chromium, nickel, molybdenum and manganese. This graph shows that the thermodynamic tendency of formation for these chlorides is very low (less than  $10^{-9}$ ).

According to Fig. 1b, there are no chlorination problems in the substrate and there should not be corrosive attack by HCl in the process of formation of aluminum coating under the selected deposition conditions. The reactions of formation of aluminum chlorides are more favored than chlorination reactions of the substrate. In the thermodynamic simulation were obtained the potential solid phases which are expected to take place during the deposition of aluminum on both austenitic stainless steels. The simulation was carried out at a temperature range from 500 to  $660^\circ C$  as shown in Fig. 2a, where the solid phases present in the deposition are BCC\_A2-2,  $Al_2Fe$  and  $Al_3Ni_2$  in smaller proportion. The compound BCC\_A2-2, is formed by  $Fe_{0.554} Al_{0.262} Cr_{0.162} Mn_{0.012} Mo_{0.007}$ .  $Al_2Fe$  has a large mass decrease at the whole range of temperature. The greatest amount of molybdenum is in steel AISI 316 form the phase BCC\_A2-1, this phase containing

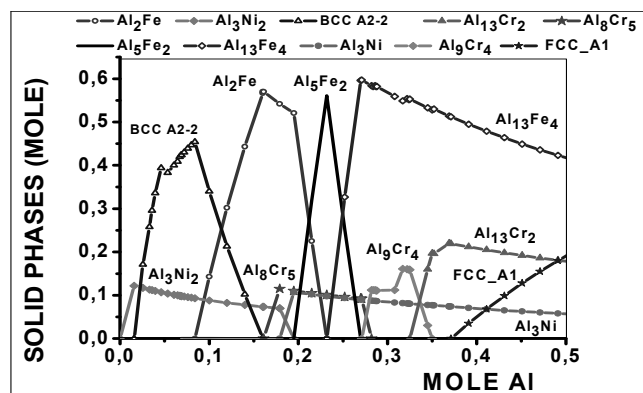
$Mo_{0.9939}Cr_{0.0043}Al_{0.0011}Mn_{0.0004}$  and it is very small, also decreases slightly at the whole range of temperature.

Fig. 2b shows the simulation thermodynamics of solid phases that might be encountered during the deposition of aluminum based on the moles of aluminum on austenitic stainless steels. The same solid phases reported in thermodynamic simulation Fig. 2a are present at the beginning of Fig. 2b, namely BCC\_A2-2,  $Al_2Fe$  and  $Al_3Ni_2$ . As the concentration of aluminum moles increases, new solid phases arise containing higher aluminum content such as  $Al_5Fe_2$ ,  $Al_8Cr_5$ ,  $Al_3Ni$ ,  $Al_{13}Fe_4$ ,  $Al_9Cr_4$  and  $Al_{13}Cr_2$ . BCC\_A2-2 phase consists of  $Fe_{5.01}Ni_{3.83}Cr_{0.55}Mo_{0.008}Mn_{0.004}$  in the coating on steel AISI 316 and in the coating on steel AISI 304 is composed of  $Fe_{4.8}Ni_4Cr_{0.55}Mn_{0.005}$ .

Pre-eliminate tests were conducted in the CVD-FBR reactor using a bed formed by a 10 % aluminum powder and 90 % bed inert (alumina), it was fluidized with argon and a mixture of gases HCl/ $H_2$  as activators. The argon flow was varied from 50 % to 80 % and the relation of gas activators from 1/15 to 1/20. For HCl/ $H_2$  relations under 1/20, uniform aluminum coatings were not obtained, since there is only a small change in tone of the surface of the substrate and also the cross sections reveal "islands" of aluminum coating after surface analysis in the microscope. For relations greater than 1/16.5 HCl/ $H_2$  begins to chlorinate the aluminum coating at temperatures above  $580^\circ C$ . This was done in order to find good conditions of aluminum deposition on the two stainless steels.



a) Solid species in function of temperature.



b) Solid species in function of aluminum.

Figure 2. Thermodynamic simulation of aluminum deposition process on austenitic stainless steels. CVD-FBR deposition process. Source: The Authors

The aluminum deposition is achieved with the following relations: concentration of active gas HCl/H<sub>2</sub> from 1/20 to 1/16.5; with gas flows as follows active gas (HCl/H<sub>2</sub>) from 44 % to 34 % and argon from 56 % to 66 %. The best deposits are achieved in the early stages of fluidization of the bed, since it has a fluid bed with a low flow gas. The best coatings were obtained with 61% of argon, 37.1% hydrogen and 1.9% of hydrochloric acid, in bed with 90% alumina and 10% aluminum powders. Therefore, under these conditions temperature varied from 560 to 600°C and deposition times from 45 to 150 minutes, to assess how the thickness of the deposited layer varies with the change of these variables.

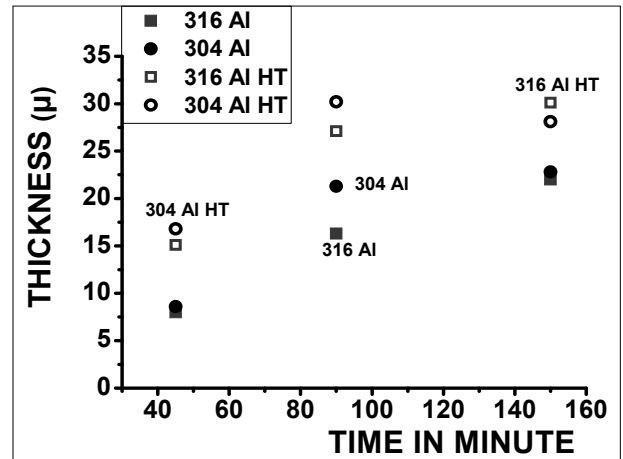
Fig. 3a shows the thickness changes during time of exposure at 580 °C, for specimens coated with and without heat treatment. Heat treatment was performed at 750 °C for two hours. Fig. 3b shows the thickness change versus exposure temperature for 1.5 hours deposition time, for specimens coated with and without heat treatment. Heat treatment was performed at 750 °C for two hours. The aluminum coating thickness increases when increasing temperature up to 580 °C. For steel AISI 316, the thickness increase is slower from 580 to 600 °C, but for steel AISI 304 thickness decreases from 580 to 600 °C. In addition, at 600 °C is observed the chlorine peak in EDAX analysis, indicating that the coating is starting to chlorinate; for this reason the deposition temperature was fixed at 580 °C from this point on.

The aluminum coating thickness increases with increase deposition time, in the first 90 minutes in an accelerated way, then the increase in thickness is slower, for this reason the deposition time was fixed at 90 minutes from this point on, since the thickness gain is very small in the remaining 60 minutes of exposure, thus it is advisable to stop CVD-FBR at this point, because the costs from the use of inert and reactive gases are avoided for 60 minutes of exposure. The coating characteristics like the thickness and homogeneity depend strongly on the input ratio of active and inert gases (HCl/H<sub>2</sub>, Ar respectively), as well as on temperature and time. The thickness of samples is correlated to increase of the equilibrium partial pressure of gaseous precursors, due to the increase of the partial pressure of precursors, also cause more interaction of precursors with the substrate and thus forming a greater amount of aluminum coating.

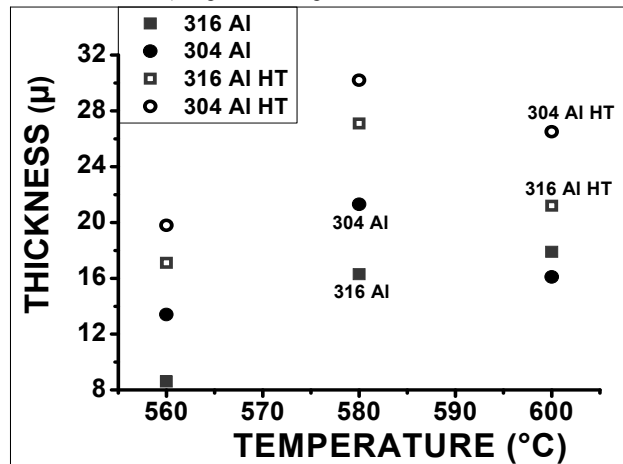
Fig. 4 shows the surface of aluminum coatings on AISI 304 stainless steels, in which there was a slight conical growth of this coating, also it is possible to see that the cones have some flake-like projections. In the early stages of deposition in different points of the sample, round nodules are formed, whose upward growth is faster than their sideways growth, leading to the formation of these conical forms and as time goes on, these cones collide with each other. Subsequently they cover the whole sample surface.

Generally, the growth of the layer can be controlled by a surface process reaction-diffusion. The lateral growth is more difficult on the base of cones, because there is more chromium on the substrate. Keep in mind that chromium does not help the growth of inter-metallic aluminum; so it is easier that the layer grow upwards than grows sideways. The coatings surface composition analysis by EDAX report:

almost 50 % aluminum, 25 % iron, 12 % chromium, 10 % nickel, 1% manganese and small amounts of molybdenum 0.65 % for the AISI 316 stainless steel.



a) Deposition temperature at 580°C.



b) Deposition time 1.5 hours.

Figure 3. Thickness of aluminum coatings on both stainless steels. Source: The Authors

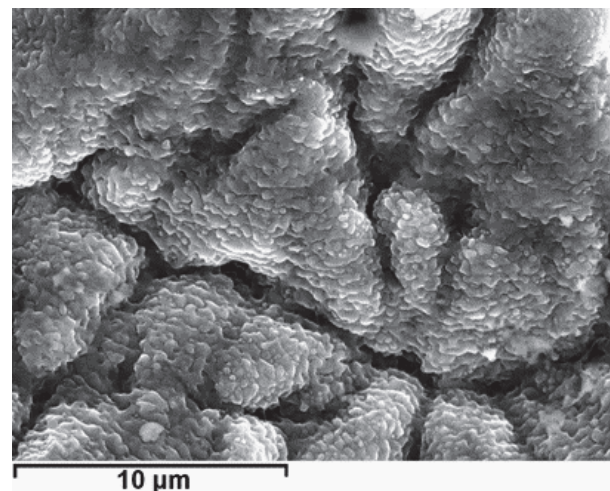
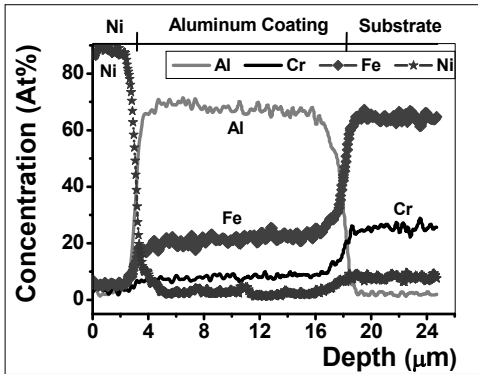
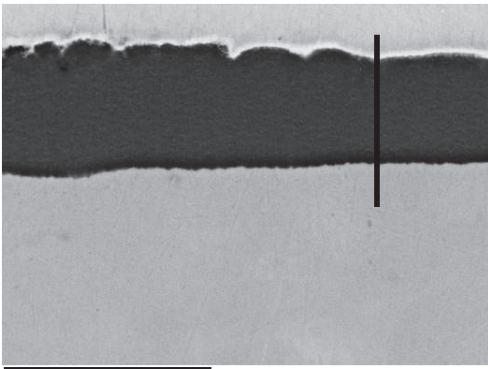
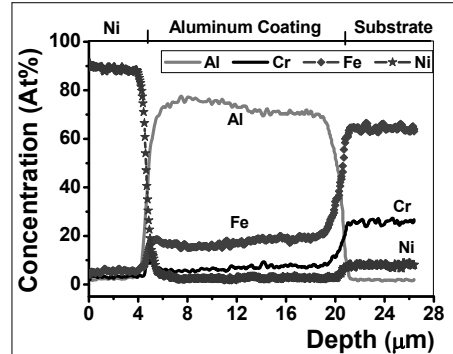
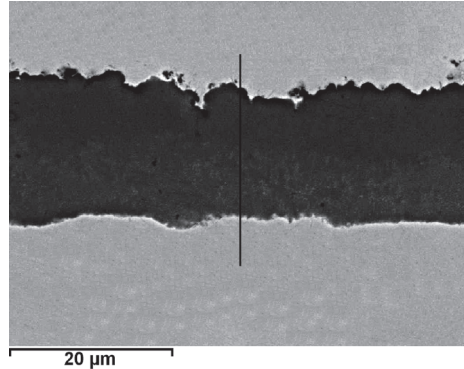


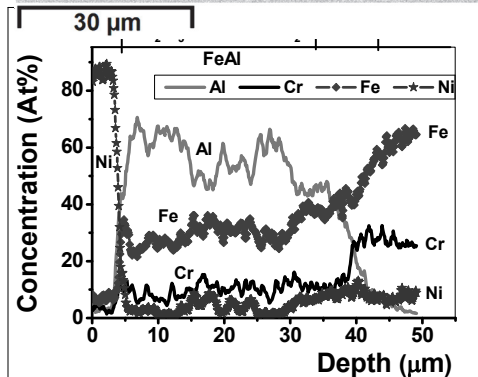
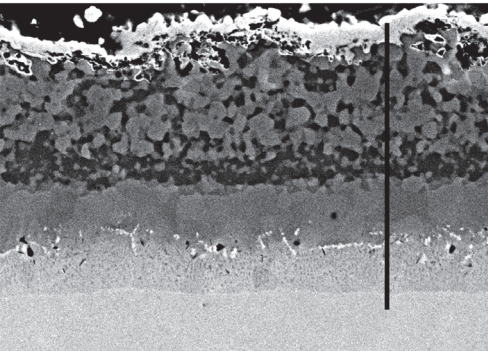
Figure 4. Surface of the aluminum coatings on stainless steels AISI 304. Source: The Authors



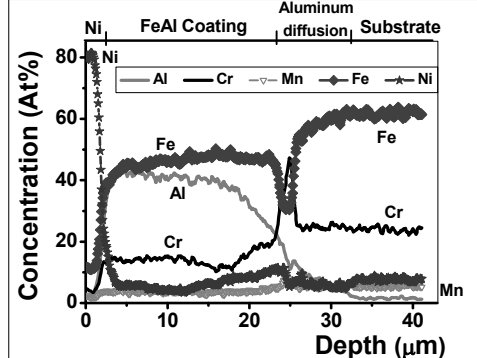
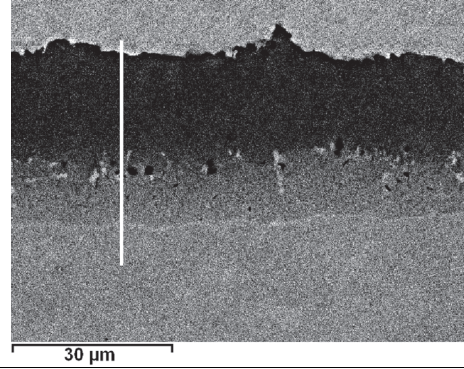
a) Stainless steel AISI 304 aluminum coated without heat treatment.



c) Stainless steel AISI 316 aluminum coated and without heat treatment.



b) Stainless steel AISI 304 aluminum coated and heat treated.



d) Stainless steel AISI 316 aluminum coated and heat treated.

Figure 5. Cross section of aluminum coating on the stainless steel AISI 304 and AISI 316. Source: The Authors

In the process of aluminum deposition by CVD-FBR homogeneous coatings were obtained with a variation of +/- 5 microns in thickness. Cross sections presented in Fig. 5,

show that the aluminum amount is higher in the coating surface and decreases slightly toward the substrate-coating interface. The iron and chromium have greater percentages

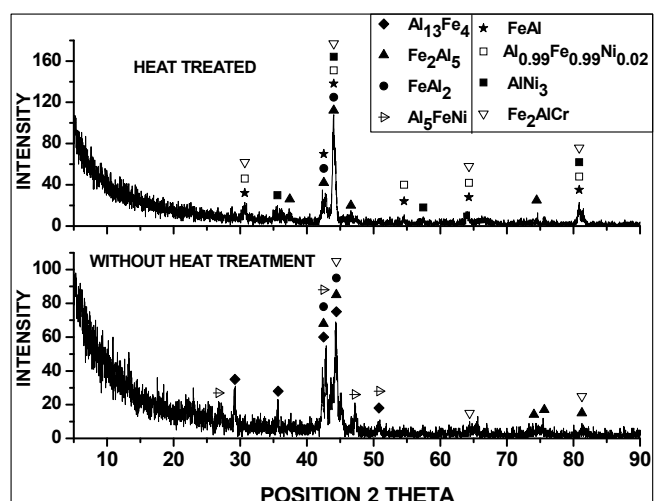
in the interface coating-substrate than in surface-coating. Nickel is homogeneously distributed through the coating. Heat treatment was conducted in these coatings to improve oxidation resistance. It was observed that aluminum diffuses into the substrate and the coating has a mixture of  $\text{Fe}_2\text{Al}_5$ ,  $\text{FeAl}_2$  and  $\text{FeAl}$  among other compounds, this is shown in analyses of X-ray diffraction (Fig. 6). Also it is observed a zone of  $\text{FeAl}$  in the interface coating-substrate. Fig. 5 shows the cross section for these aluminum coatings with and without heat treatment, to see how the coating composition varies depending on the heat treatment. Non-heat treated coating are composed approximately of 67% aluminum, 20% iron, 8% chromium and 5% nickel and heat treated coating are composed approximately of 50% aluminum, 34% iron, 10% chromium and 6% nickel.

Fig. 5b shows that aluminum-coated AISI 304 steel presents four zones: an external rich in  $\text{FeAl}_2$  and  $\text{Fe}_2\text{Al}_5$ , with some parts darker than the others, the second area rich in  $\text{FeAl}$ , the third area rich in chromium, containing a band of  $\text{Fe}_2\text{AlCr}$  and finally the area of aluminum diffusion in the substrate. Fig. 5d shows that aluminum-coated AISI 316 steel presents three zones: an external zone corresponding to the coating that after heat treatment is formed mainly  $\text{FeAl}$ , this zone has 18  $\mu\text{m}$  approximately, between the coating and the substrate there is a chromium-rich band, which should contain  $\text{Fe}_2\text{AlCr}$ , even though this band cannot be noticed by naked eye, it was observed in the composition line analysis. The other zone is formed by diffusion of aluminum on the material base, in this area we can see the Kirkendal effect [9-19], since there are numerous pores generated by inter diffusion of aluminum and iron.

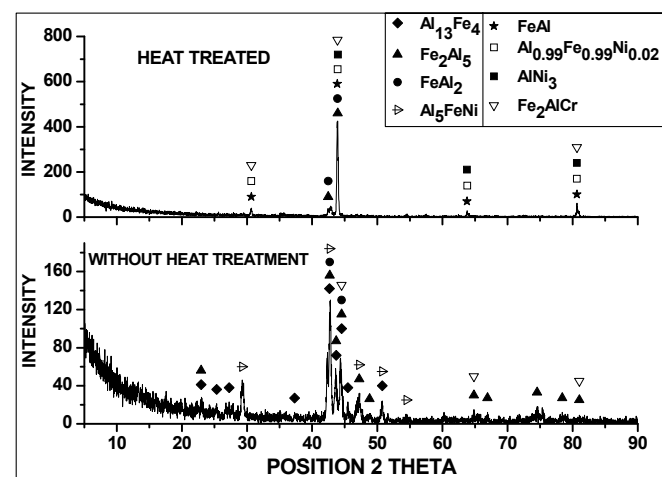
In Fig. 6 are showed the analyses of X-ray diffraction (XRD); the coatings without heat treatment are formed by  $\text{Al}_{13}\text{Fe}_4$ ,  $\text{Fe}_2\text{Al}_5$ ,  $\text{FeAl}_2$  and  $\text{Al}_5\text{FeNi}$  for the two steels. In addition, the heat treatment transformed the above components to form the  $\text{FeAl}$ ,  $\text{Fe}_2\text{Al}_5$ ,  $\text{Al}_{0.99}\text{Fe}_{0.99}\text{Ni}_{0.02}$ ,  $\text{AlNi}_3$  and the  $\text{Fe}_2\text{AlCr}$ . This is corroborated with the line analysis performed by EDAX to coatings with and without heat treatment, besides the heat treatment reduces the amorphous characteristic of the structure of the aluminum coatings. Heat treatment favored the transformation of aluminum-rich phases into others with greater iron content, due to inter diffusion of aluminum, iron and chromium. It is clear that aluminum diffuses into the substrate faster than iron diffuses into the coating, since the diffusion coefficient of aluminum is an order of magnitude greater than that of the iron [19]. This aids to improve mechanical properties and corrosion resistance of the coating.

### 3.2. Steam oxidation

The specimens were exposed at 750 °C in a steam loop to assess the degree of protection provided by these coatings under supercritical temperature and in an aggressive environment. Both uncoated substrates behaved differently, since the steel AISI 304 performed well and gained low mass, whereas steel AISI 316 lost too much weight. Coated steels gained little weight during the thousand hours of exposure and are highly resistant to oxidation. Gravimetric



a) Aluminum coating on AISI 304 stainless steel

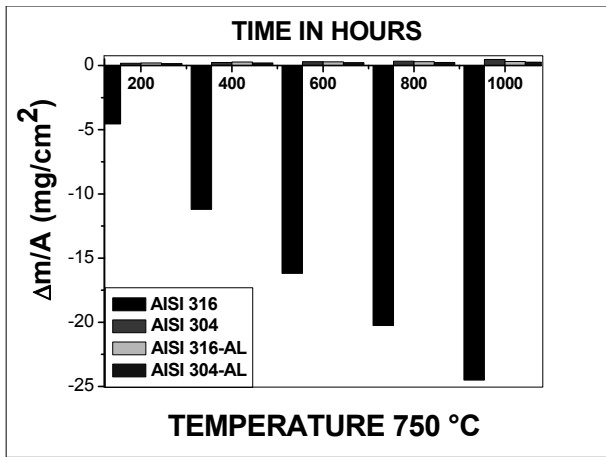


b) Aluminum coating on AISI 316 stainless steel

Figure 6. Analysis of X-ray diffraction for the coatings on AISI 304 stainless steel and AISI 316 stainless steel.

Source: The Authors.

measurements have confirmed that the application of these aluminium coatings on austenitic stainless steels by CVD-FBR allows to reduce the oxidation rate more than 80 times under super critical conditions. When the corrosive attack begins, the coated steel gained mass at higher speed, it happens in the first 400 hours and then mass gain decelerates, because aluminum coating has good resistance to oxidation in oxidizing environments; because it forms a surface layer of  $\text{Al}_2\text{O}_3$ , with oxides rich in chromium and nickel, this layer is compact and adherent and protects the coating from corrosive attack [20,21]. Uncoated steels show a linear attack for the whole time. The corrosion rate of the AISI 304 steel has a tendency to increase over time, whereas the AISI 316 steel has a great weight loss, because the oxide layer formed in the early hours grows quickly and then falls, leaving the substrate exposed to corrosive attack and the corrosion process continues.



a) The entire range of mass gain.

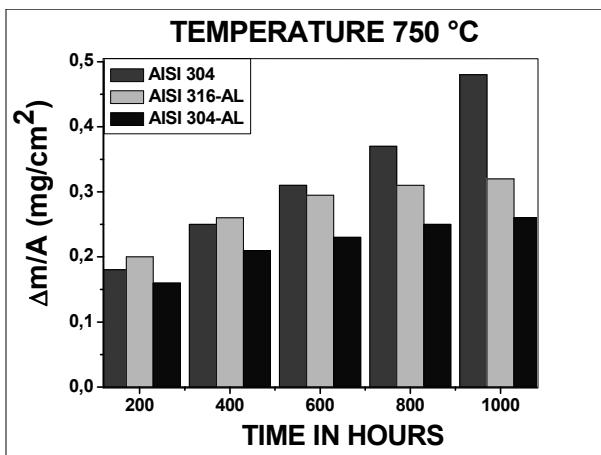
b) Mass gain from 0 to 0.5 mg/cm<sup>2</sup>

Figure 7. Mass gain of stainless steel with aluminum coated and uncoated oxidized in the loop steam at 750 °C.

Source: The Authors.

During the initial oxidation, elements more active than iron react and form oxides; as aluminum is the most reactive, this will be the first to react with oxygen to form  $Al_2O_3$ , followed by the chromium forming  $Cr_2O_3$ , once the alumina layer is formed, the  $Cr_2O_3$  is dissolved in the layer or evaporates. Moreover the corrosion resistance also depends on the thickness of the layer [22,23]. Degradation of the chromite layer by volatile compounds formation takes place when the chromite layer ( $Cr_2O_3$ ) interacts with water vapour, producing chromium hydroxides like  $(CrO_2(OH)_2)_{(g)}$  or  $CrO_2(OH)_{(g)}$  [24,25]. Aluminum coatings are highly protective at high oxidation temperatures, in comparison to uncoated stainless steels substrates because the oxidation rate decreases several orders of magnitude, as it is shown in Fig. 7. Aluminum coating does not form the  $Fe_2O_3$  nor  $Fe_3O_4$ , thus the coating prevents the formation of  $FeO$ . The aforementioned iron oxides have a very limited protective capacity [26,27]. The results showed that aluminum coating have a beneficial effect in the protection of austenitic stainless steels in steam oxidizing conditions at super critical temperatures (over 700 °C), as these coatings significantly reduce the corrosion rate, making these

coatings a good alternative to protect steels in super critical conditions for future applications in power plants.

The thermodynamic simulation is a good tool to select the working conditions and identify the aluminum halides performing the deposition of aluminum. In the simulation of solid compounds the only species present in the coating was  $FeAl_2$ . Furthermore, it is possible that Cr is present in solid solution in the intermetallic phases, since the substrate contains Cr and the structures of these intermetallic phases are not affected by the introduction of Cr [28]. On the other hand, EDX analysis shows that chromium is also in aluminum coating. In the literature, X-ray diffraction reported that during the deposition of aluminum in stainless steels, Cr diffuses readily into the coating to form mainly  $Cr_5Al_8$  on the outer surface [29], however XRD results of this study do not show the formation of this compound.

#### 4. Conclusions

- The CVD-FBR is an effective technique to obtain very uniform and homogeneous aluminum coatings on austenitic stainless steels at low temperature, short time and atmospheric pressure; furthermore aluminum coatings of more than 20  $\mu m$  of thickness can be obtained.
- To obtain aluminum coatings of 20  $\mu m$  the deposition conditions by CVD-FBR were improved at temperatures below 600 °C, without affecting the microstructure of austenitic stainless steels. Furthermore, the behavior of these coatings in steam oxidation conditions is significantly better than that observed on uncoated substrates. CVD-FBR is an important alternative to improve steam oxidation resistance of austenitic stainless steels. Yielding great chances to shorten times and lower costs.
- The aluminum coating deposited by CVD-FBR without heat treatment forms inter metallic compounds with iron such as  $Al_{13}Fe_4$ ,  $Fe_2Al_5$ ,  $FeAl_2$  and  $Al_5FeNi$ . Subsequently they are transformed by diffusion heat treatment into  $FeAl$ ,  $Fe_2Al_5$ ,  $Al_{0.99}Fe_{0.99}Ni_{0.02}$ ,  $AlNi$  and  $Fe_2AlCr$ , and as a result oxidation resistance of the substrate is improved. Furthermore the coating expands after heat treatment due to the inter diffusions of iron and chromium outward and the aluminum into the substrate, thereby the coating can reach up to 35  $\mu m$  of thickness.
- Aluminum deposited on the coating form alumina on the surface that acts as a barrier against oxidation. Therefore, the aluminum coating is able to extend the life of stainless steel AISI 304 and AISI 316 under steam oxidation at 750 °C.

#### Acknowledgements

The authors would like to thank Departamento Administrativo de Ciencia, Tecnología e Innovación - COLCIENCIAS for his doctoral fellowship and Universidad Tecnológica de Pereira for the study commission. The research group would like to thank the Spanish Ministry of Science for its contribution to this paper: Project MICINN ENE 2008-06755-C02-02 and

CONSOLIDER CSD 2008-00023.

**5. References**

- [1] Trevisan, R. y Lima, C., *Aspersao Termica Fundamentos E Aplicacoes*. Editorial Artliber. Brazil, 2002.
- [2] Marulanda-Arévalo, J.L., Castañeda-Quintana, S.I. and Remolina-Millan, A., Coatings deposited by CVD-FBR for protection at high temperature. *DYNA*, 80 (181), pp. 181-191, 2013.
- [3] Garcia, D., Piratoba, U. and Mariño, A., (Ti,Al)N Coatings on AISI 4140 by R.F. sputtering. *DYNA*, 74 (152), pp. 181-185, 2007.
- [4] Bolívar, F.J., Sánchez, L., Tsipias, S.A., Hierro, M.P., Trilleros, J.A. and Pérez, F.J., Silicon coating on ferritic steels by CVD-FBR technology, *Surface & Coatings Technology*, 201 (7), pp. 3953-3958, 2006. <http://dx.doi.org/10.1016/j.surfcoat.2006.08.101>
- [5] Brossard, J.M., Hierro, M.P., Sánchez, L., Bolívar, F.J. and Pérez, F.J., Thermodynamical analysis of Al and Si halide gaseous precursors in CVD. Review and approximation for deposition at moderate temperature in FBR-CVD process, *Surface & Coatings Technology*, 201 (6), pp. 2475-2483, 2006. <http://dx.doi.org/10.1016/j.surfcoat.2006.04.018>
- [6] Choy, K.L., Chemical vapour deposition of coatings, *Progress in Materials Science*, 48 (2), pp. 57-170, 2003. [http://dx.doi.org/10.1016/S0079-6425\(01\)00009-3](http://dx.doi.org/10.1016/S0079-6425(01)00009-3)
- [7] Oura, K., Lifshits, V., Saranin, A., Zotov, A. and Katayama, M., *Surface Science. An Introduction*, Germany 2003. <http://dx.doi.org/10.1007/978-3-662-05179-5>
- [8] Pérez, F.J., Pedraza, F., Hierro, M.P. and Hou, P.Y., Adhesion properties of aluminide coatings deposited via CVD in fluidised bed reactors (CVD-FBR) on AISI 304 stainless steel, *Surface & Coatings Technology*, 133-134, pp. 338-343. 2000. [http://dx.doi.org/10.1016/S0257-8972\(00\)00952-X](http://dx.doi.org/10.1016/S0257-8972(00)00952-X)
- [9] Bolivar, F.J., Pérez, F.J., Hierro, M.P., Trilleros, J.A. y Sánchez, L., Aluminización de aceros ferríticos-martensíticos (hcm-12a) mediante CVD-FBR, *Scientia et Technica*, 36, pp. 619-624. 2007.
- [10] Chaliampalias, D., Vourlias, G., Pistofidis, N., Pavlidou, E., Stergiou, A. and Stergioudis, G., Deposition of zinc coatings with fluidized bed technique, *Materials Letters*, 61 (1), pp. 223-226, 2007. <http://dx.doi.org/10.1016/j.matlet.2006.04.036>
- [11] Voudouris, N., Christoglou, Ch. and Angelopoulos, G., Formation of aluminide coatings on nickel by a fluidised bed CVD process, *Surface and Coatings Technology*, 141 (2-3), pp. 275-282, 2001. [http://dx.doi.org/10.1016/S0257-8972\(01\)01193-8](http://dx.doi.org/10.1016/S0257-8972(01)01193-8)
- [12] Christoglou, Ch., Voudouris, N. Angelopoulos, G.N. Pant, M. and Dahl, W., Deposition of aluminium on magnesium by a CVD process, *Surface and Coatings Technology*, 184 (2-3), pp. 149-155, 2004. <http://dx.doi.org/10.1016/j.surfcoat.2003.10.065>
- [13] Pérez, F.J., Hierro, M.P., Pedraza, F., Carpintero, M.C., Gómez, C. and Tarín, R., Effect of fluidized bed CVD aluminide coatings on the cyclic oxidation of austenitic AISI 304 stainless steel, *Surface and Coatings Technology*, 145 (1-3), pp. 1-7, 2001. [http://dx.doi.org/10.1016/S0257-8972\(01\)01019-2](http://dx.doi.org/10.1016/S0257-8972(01)01019-2)
- [14] Christoglou, Ch., Voudouris, N. and Angelopoulos, G.N., Formation and modelling of aluminide coatings on iron by a fluidised bed CVD process, *Surface and Coatings Technology*, 155 (1), pp. 51-58, 2002. [http://dx.doi.org/10.1016/S0257-8972\(02\)00044-0](http://dx.doi.org/10.1016/S0257-8972(02)00044-0)
- [15] Anastassiou, C., Christoglou, C. and Angelopoulos, G.N., Formation of aluminide coatings on Ni and austenitic 316 stainless steel by a low temperature FBCVD process, *Surface & Coatings Technology*, 204 (14), pp. 2240-2245, 2010. <http://dx.doi.org/10.1016/j.surfcoat.2009.12.018>
- [16] Hao-Tung L., Sheng-Chang W., Jow-Lay H., Shin-Yun Ch. Processing of hot pressed Al<sub>2</sub>O<sub>3</sub>-Cr<sub>2</sub>O<sub>3</sub>/Cr-carbide nanocomposite prepared by MOCVD in fluidized bed, *Journal of the European Ceramic Society*, 27 (16), pp. 4759-4765. 2007. <http://dx.doi.org/10.1016/j.jeurceramsoc.2007.02.207>
- [17] Andersson, J.O., Helander, T., Hoglund, L.H., Shi, P.F. and Sundman, B., CALPHAD: Comput. Coupling Phase Diagrams *Thermochem*, 26. 273 P. 2002.
- [18] Pérez, F.J., Hierro, M.P., Pedraza, F., Gómez, C., Carpintero, M.C. and Trilleros, J.A., Kinetic studies of Cr and Al deposition using CVD-FBR on different metallic substrates, *Surface and Coatings Technology*, 122 (2-3), pp. 281-289, 1999. [http://dx.doi.org/10.1016/S0257-8972\(99\)00305-9](http://dx.doi.org/10.1016/S0257-8972(99)00305-9)
- [19] Pérez, F.J., Hierro, M.P., Trilleros, J.A., Carpintero, C., Sánchez, L., Brossard, J.M. and Bolívar, F.J., Iron aluminide coatings on ferritic steels by CVD-FBR technology, *Intermetallics*, 14 (7), pp. 811-817, 2006. <http://dx.doi.org/10.1016/j.intermet.2005.12.010>
- [20] Kobayashi, S. and Yakou T., Control of intermetallic compound layers at interface between steel and aluminum by diffusion-treatment, *Materials science and engineering: A*, 338 (1-2), pp. 44-53, 2002. [http://dx.doi.org/10.1016/S0921-5093\(02\)00053-9](http://dx.doi.org/10.1016/S0921-5093(02)00053-9)
- [21] Smialek J.L. and Auping J.V., COSP for Windows—Strategies for Rapid Analyses of Cyclic-Oxidation Behavior, *Oxidation of Metals*, 57 (1-2), pp. 559-581, 2002. <http://dx.doi.org/10.1023/A:1015308606869>
- [22] Hong-yan, D., Zhen-dong, D., Suresh-C.S., David H., Corrosion wear behaviors of micro-arc oxidation coating of Al<sub>2</sub>O<sub>3</sub> on 2024Al in different aqueous environments at fretting contact, *Tribology International*, 43 (5-6), pp. 868-875, 2010. <http://dx.doi.org/10.1016/j.triboint.2009.12.022>
- [23] Babu, N., Balasubramaniam, R. and Ghosh, A., High-temperature oxidation of Fe<sub>3</sub>Al-based iron aluminides in oxygen, *Corrosion Science* 43 (12), pp. 2239-2254, 2001. [http://dx.doi.org/10.1016/S0010-938X\(01\)00035-X](http://dx.doi.org/10.1016/S0010-938X(01)00035-X)
- [24] Castañeda, S.I., Bolívar, F.J. and Pérez, F.J., Study of Oxyhydroxides Formation on P91 Ferritic Steel and CVD-FBR Coated by Al in Contact with Ar + 40% H<sub>2</sub>O at 650 °C by TG-Mass Spectrometry, *Oxidation of metal*, 74 (1-2), pp. 61-78, 2010. <http://dx.doi.org/10.1007/s11085-010-9200-z>
- [25] Marulanda, J.L., Pérez, F.J. and Castañeda, S.I., Aluminum-silicon coatings on austenitic stainless steel (AISI 304 and 317) deposited by chemical vapor deposition in a fluidized bed, *Ingeniería e Investigación*, 34 (2), pp. 5-10, 2014. <http://dx.doi.org/10.15446/ing.investig.v34n2.41249>
- [26] Paul, A., Odriozola, J.A Development of a modified CVD coating process for the enhancement of the high temperature oxidation resistance of Cr<sub>2</sub>O<sub>3</sub> and Al<sub>2</sub>O<sub>3</sub> forming alloys, *Materials Science and Engineering:A*, 300 (1-2), pp. 22-33, 2001. [http://dx.doi.org/10.1016/S0921-5093\(00\)01802-5](http://dx.doi.org/10.1016/S0921-5093(00)01802-5)
- [27] Huttunen-Saarivirta, E., Stott, F.H., Rohr, V. and Schutze, M., Particle angularity effects on the elevated-temperature erosion-oxidation behaviour of aluminium diffusion coatings on 9% Cr steel, *Wear*, 261 (7-8), pp.746-759. 2006. <http://dx.doi.org/10.1016/j.wear.2006.01.014>
- [28] Palm, M., The Al-Cr-Fe system—Phases and phase equilibria in the Al-rich corner, *Journal of Alloys and Compounds*, 252 (1-2), pp. 192-200, 1997. [http://dx.doi.org/10.1016/S0925-8388\(96\)02719-3](http://dx.doi.org/10.1016/S0925-8388(96)02719-3)
- [29] Dumitrescu, L. and Maury, F., Al<sub>2</sub>O<sub>3</sub> coatings on stainless steel from Al metal-organic chemical vapor deposition and thermal treatments, *Surface and Coating Technology*, 125 (1-3), pp. 419-423, 2000. [http://dx.doi.org/10.1016/S0257-8972\(99\)00616-7](http://dx.doi.org/10.1016/S0257-8972(99)00616-7)

**J.L. Marulanda-Arévalo**, is Professor at the Universidad Tecnológica de Pereira. Pereira-Colombia. Metallurgical Engineer in 1999 and MSc. in Metallurgical Engineering in 2002, from the Universidad Industrial de Santander. Colombia. PhD. in Advanced Chemistry, from the Universidad Complutense de Madrid. España.

**F.J. Pérez-Trujillo**, is profesor at the Universidad Complutense de Madrid. Madrid-España. Degree in Chemistry and Industrial Engineer, all of them from the Universidad Complutense de Madrid. España, is PhD. in Chemical Sciences, *University of California, Los Angeles. USA.*

**S.I. Castañeda-Quintana**, is Researcher at the Universidad Complutense de Madrid. Madrid-España. Degree in Physics and MSc. in Physical Sciences, all of them from the Universidad Nacional Mayor de San Marcos, Lima-Perú. Ph.D. in Physical Sciences, from the Universidad Autónoma de Madrid, España.